



UNIOSUN Journal of Engineering and Environmental Sciences. Vol. 4 No. 1. March. 2022

Archachatina marginata Snail-shell as a Feedstock for the Synthesis of Solid Catalysts for Methanolysis of Oil from Palm Kernel in an Optimisation Process

Ajala, E.O., Ajala, M.A., Agbeleoba, E.D., Odetoye, T.E., Eromonsele, O.P. and Ayanshola, A.M.

Abstract: The work studied the synthesis of heterogeneous catalysts from *Archachatina marginata*s nail-shell (AMS) by calcination at 800°C and 900°C for 2 h, to produce snail shell catalyst (SSC) of SSC800 and SSC900 respectively. The catalysts were subsequently used for palm kernel biodiesel (PKB) production using palm kernel oil (PKO) in an optimisation study using a definitive screening design. The AMS, SSC800 and SSC900 were characterised by Atomic Absorption Spectrophotometer (AAS), Brunauer-Emmett-Teller (BET) and Scanning Electron Microscopy (SEM). The AAS result revealed that the catalysts contained essential elements of Ca, Mg, Na, Si and K which are suitable for transesterification reactions in proportion of 66.67%, 1.12%, 2.06%, 3.01% and 9.33% for SSC800 respectively, and 59.33%, 1.03%, 2.30%, 2.50% and 8.00% for SSC900 respectively. The images of the catalysts revealed improved surface morphologies with larger porosities compared to that of the AMS, having surface areas of 244.2 m²/g and 230.9 m²/g for SSC800 and SSC900respectively. This justified the reason for the higher catalytic activity of the SSC800 compared to the SSC900. The optimisation study gave the optimal conditions for the optimum biodiesel vield of 98.28% as 6:1 MeOH: oil molar ratio, 3 h reaction time, 55°C temperature and 2% (w/w) catalyst quantity of SSC800. The fuel properties obtained for the PKB compared well with the ASTM standard of biodiesel and as such, it is a quality biodiesel suitable for compression ignition engines. Therefore, the Archachatina marginata snail-shell is an effective, suitable, natural and renewable material for catalysts development for commercial biodiesel production.

Keywords: Archachatina marginata, Biodiesel, Catalyst, Characterisation, Optimisation, Snailshell

I. Introduction

An increase in world population, rapid industrialisation, urbanisation as well as unsustainable extraction and utilisation of fossil fuels have caused a reduction in crude reserve, environmental deterioration and global warming[1–4]. The threats of fossil fuels to human existence have led to the search for an alternative, sustainable and renewable energy source which has increased

the devotion of scientists to the synthesis of biodiesel for compression ignition engines [5].

Nowadays, biodiesel is a known carbonneutral, bio-degradable, sulphur-free, nontoxic, renewable and environmentally benign source of bioenergy [6]. Biodiesel is usually synthesised by the alcoholysis reaction of triglycerides (TG). The TG are either vegetable oils or animal fats and could be reacted with short-chain alcohol (methanol or ethanol), in the presence of a catalyst to form biodiesel [7]. The catalysts for the alcoholysis either homogeneous reaction heterogeneous and are often defined as substances that accelerate the chemical reaction processes. Kaewdaeng et al. [8] reported that the homogeneous catalytic process has high yields of biodiesel and quick reaction time but has some drawbacks. The

Ajala, E.O., Ajala, M.A., Agbeleoba, E.D., Odetoye, T.E., Eromonsele, O.P. (Department of Chemical Engineering, University of Ilorin, Kwara State, Nigeria

Ayanshola, A.M. (Department of Water Resources and Environmental Engineering, University of Ilorin, Kwara State, Nigeria)

Corresponding author: ajala.oe@unilorin.edu.ng

Phone Number: +2348034401203

Submitted: 22-12-2021 Accepted: 22-01-2022 drawbacks include the of generation wastewater purification, from corrosion tendencies, non-ecological and non-reusability of the catalysts, development of emulsions, difficulty in eliminating the catalyst used and its subsequent disposal [6, 9]. To overcome aforementioned the challenges catalysts, a heterogeneous homogeneous catalytic process could be an option. Heterogeneous catalysts are easy to separate from the reaction mixture, their usage decreases the quantity of wastewater from the process and are usually reusable.

Calcium oxide (CaO) is an example of a heterogeneous catalyst that is widely recognised as a highly active catalyst due to its high basic strength [8]. Apart from the aforementioned advantages of the CaO based catalyst for biodiesel production, it is cheaper and can be obtained from many natural sources that contain calcium carbonate. Examples of such natural sources are waste obtuse horn, natural rocks (calcite and dolomite), hydrated lime, waste coral fragment and chicken bones [5, 7]. Other sources of CaO for heterogeneous catalysts development for biodiesel production are chicken eggshell, river snail-shell and crab shell [10], shellfish and mollusc [6], oyster shells and sea sand [2], crab shells, ostrich eggshells, capiz shells and clamshells [11].

Recently, chicken eggshell was processed into solid catalysts for methanolysis of PKO and chicken fat for biodiesel production of 97.10% and 90.2% yield respectively and was proven to have strong reusability capability with no loss of activity [12, 13]. These show that the chicken eggshell can serve as a cheap feedstock for a heterogeneous catalyst that can yield more than 95% biodiesel. As the catalyst produced from the natural waste shells open doors for economic advancement, environmental recovery and sustainable utilisation of wastes, simultaneously [6]. The

catalyst from CaO sources is an auspicious and cheap candidate for the impending industrial-scale production of biodiesel [14]. Although an extensive study has been reported on the usage of CaO from different derivations for the production of biodiesel, little information is available on the utilisation of CaO from snail shells of *Archachatina marginata* for biodiesel production using PKO.

The Archachatina marginata snail is a family of Phylum mollusca which has the most species (>100,000) inhabiting the earth after arthropods and plays significant roles in ecosystems. The snail is edible for human beings, crabs and birds, and their productivity is accompanied by various food chains [15].

It was reported that geographical location and environmental conditions can influence shell morphology and size of snails in an ecosystem, this provoked scholars to explore the characteristics of the shells [15, 16]. The Archachatina marginata snail-shell (AMS) is composed of mainly CaCO3 which encloses, supports and protects the soft part of the animal [17]. It is also made up of magnesium, potassium, iron, chloride sodium phosphorus [18]. The presence of these vital chemical elements indicates that the AMS is a suitable raw material to synthesise biodiesel heterogeneous catalysts for production.

Otori et al. [19] synthesised CaO solid catalyst using AMS as a precursor and was used for biodiesel production of 85% yield from Afzelia Africana seed oil. The characterisations of the catalysts developed were not adequately investigated and the process was not optimised using any model. The AMS derived solid catalyst was also developed to produce biodiesel using soybean oil and achieved a yield of 98% [15]. The reaction time for the process indicated 7 h, which was very high, as the process was not optimised using any

optimisation process and the oil used was not PKO.

Gupta and Agarwal [20] synthesised CaO from the AMS for the alcoholysis of soybean oil and obtained an optimum 94% yield of biodiesel. This study reported that the CaO gave the best performance at 6% (w/w) catalyst quantity, 65°C of temperature, 9:1 of methanol to oil molar ratio (MeOH: oil ratio) and 3.5 h of reaction time. However, the study indicated that the CaO was modified by KOH to improve the activity of the catalyst, which implies an increase in the overall biodiesel production cost. Birla et al. [21] also reported that an 87.28% yield of biodiesel was successfully produced from waste frying oil in the presence of CaO catalyst from AMS. In another study, a 98.5% yield of biodiesel was attained in the presence of modified AMS by KBr-immersed and kaolin Unfortunately, the catalyst preparation is quite expensive and complex as it required the use of additional material.

Worthy of note is that in all the studies aforementioned, none utilised CaO from AMS for PKO conversion to biodiesel, not even in an optimisation study by definitive screening design, hence, the novelty of this study.

Therefore, this work aims to utilise the AMS to develop heterogeneous catalysts for PKB production. The effects of calcination temperature and other process conditions on the performance of the catalyst for PKB production was investigated in an optimisation process by a definitive screening design. The reusability of the best performing catalyst between the SSC800 and SCC900 was also investigated under optimal process conditions. The PKB produced by the best performing catalyst was tested for its physical and chemical properties, and compared with

the America Standard Testing Methods (ASTM standards) for diesel and biodiesel.

II. Materials and MethodsA. Materials

The PKO that contains 1.68% of free fatty acid used in this study was procured from a commercial source in *Obaagun*, Osun State, Nigeria. The AMS was collected from a local eatery in Ilorin Metropolis, Kwara State, Nigeria. Methanol (99.5%) and other reagents used were obtained from JHD India. A batch reactor manufactured by Armfield (USA) with model number CEXC-A, 036223-003 was used for the study.

B. Catalyst Preparation

The AMS was washed with tap water to eliminate grit and unwanted constituent from the shells. It was sun-dried to remove moisture content from the surface and crushed using a mortar and pestle. The pulverised AMS sample was screened using a <180 µm mesh size to obtain a uniform-sized product. It was then washed with 6 N HNO₃ solution thrice at 3 min each, to eliminate organic impurities, followed by rinsing with distilled water and oven-dried at 110°C for 24 h [21].

The prepared AMS sample was calcined for 2 h at various temperatures of 800°C and 900°C in a muffle furnace to produce white fluffy porous catalysts of SSC800 and SSC900 respectively. The catalysts were charged into polyethene bags and stored inside a desiccator to prevent interaction with humidity and carbon dioxide before use.

C. Characterisations of AMS and Snail Shell Catalysts of SSC800 and SSC900

The atomic absorption spectrophotometer (AAS/FP model Buck scientific Accusys 211, USA) was employed to determine the

elemental compositions of AMS, SSC800 and SSC900 samples. For the analysis, samples were digested via the Aqua Regia method using 67% HNO3 and 37% HCl in ratio 3:1 [7]. The FT-IR analysis was also carried out for each of the samples using an FT-IR Shimadzu model 8400S (USA). Brunauer-Emmett-Teller (BET) of model Nova 4200e Quantachrome (USA) was employed to measure the surface area, mean pore diameter and pore volume based on adsorption and desorption isotherm of N₂ gas. micrographs of the samples were investigated using scanning electron microscopy (SEM) coupled with Energy dispersive X-ray (EDX) of the Zeiss Auriga model.

Also, the basic strength and basicity for each sample of AMS, SSC800 and SSC900 were evaluated by the Hammett indicator method as was described by [15]. The Hammett indicators and their pKa used for the investigation are shown in Table 1. Fifty milligrams of a sample (AMS, SSC800 or SSC900) was added to 10 mL anhydrous ethanol solution of each Hammett indicator in a 250 mL beaker. The mixture was thoroughly mixed and allowed to equilibrate for 2 h. Thereafter, if the solution changes colour, it is an indication that the basic strength of the sample is higher than the Hammett indicator. However, if no colour changes are noticed, it implies that the basic strength of the sample is lower than the indicator. Each of the samples was tested with all the Hammett indicators to investigate their H range of basic sites. The basicity of the samples was equally evaluated by using the method described by [23].

A half gram (0.5 g) of the sample was measured into a 250 mL conical flask containing 50 mL deionized water and was stirred vigorously for 1 h using a magnetic

stirrer. The solution was filtered and the filtrate was titrated against an anhydrous methanol solution that contains 0.02 mol/L benzene carboxylic acid to determine the basicity of the samples.

Table 1: Hammett Indicators and their pKa Values

Hammett indicators	pKa
Bromothymol blue	7.2
Phenolphthalein	9.8
Indigo carmine	12.2
2,4- dinitroaniline	15.0
4-nitroaniline	18.4

D. Definitive Screening Design (DSD) and Data Analysis

Biodiesel production by SSC800 and SSC900 catalysts were studied in an optimisation process using the DSD (version 11.0 of SAS JMP Statistical Discovery). The experiment was designed for the optimisation study by considering process parameters of five factors at three levels as shown in Table 2. The DSD was employed to generate 18 runs of the experimental matrix using five process conditions as shown in Table 3. The %yield of biodiesel from each experimental run was taken as the response and denoted as Y (Response). The relationship between the %Yield of Biodiesel (Y) and the process conditions of MeOH: oil mole ratio, temperature, catalyst quantity, reaction time and AMS calcination temperature which were denoted as X₁, X₂, X₃, X₄and X₅respectively was proposed as a model by the DSD as shown in Equation 1:

$$Y = b_0 + b_1 X_1 + b_2 X_2 + \dots + b_n X_n + \sum_{i=1}^n b_{ik} X_i X_k + \sum_{i=1}^n b_{ii} X_i^2$$
 (1)

where; b_0 , b_1 , b_2 ... b_n are the constants.

Table 2: Definitive Screening Design Response and Process Conditions

Response Name		Goal	Lower Limit	Upper Limit
%Yield of Biodiesel		Maximize	-	-
Factors				
Name	Codes	Roles	Values	
MeOH: Oil Mole Ratio (w/w)	X_1	Continuous	6	10
Temperature (°C)	X_2	Continuous	55	65
Catalyst Quantity (w/w)	X_3	Continuous	4	8
Reaction Time (h)	X_4	Continuous	1	3
CCT (°C)	X_5	Categorical	800	900

Table 3: Experimental Matrix for the Process Conditions and Response for the DSD

Exp. Runs	MeOH: Oil Mole Ratio (w/w)	Temperature (°C)	Catalyst Quantity (%, w/w)	Reaction Time (h)	Catalyst Calcined Temperature (°C)
1	6	65	4	1	800
2	8	60	4	2	800
3	10	65	2	1	900
4	6	55	6	1	900
5	8	60	4	2	900
6	8	55	2	1	800
7	10	55	4	3	900
8	10	65	2	3	800
9	8	65	6	3	900
10	6	55	6	3	800
11	10	55	6	1	800
12	6	65	6	2	800
13	6	55	2	3	800
14	6	60	2	1	900
15	10	60	6	3	800
16	6	65	2	3	900
17	10	55	2	2	900
18	10	65	6	1	900

The multiple regression analysis of the model (Eq. 1) was developed for the response, to evaluate the linear and interaction effects of the process parameters.

The coefficient for each of the linear and interaction parameters was tested for their significance using the F and p values obtained from the analysis of variance.

E. Transesterification Reaction

The transesterification reactions of PKO and methanol in the presence of SSC800 and SSC900 catalysts were carried out in the Armfield batch reactor. The amount of catalyst to PKO of 5 wt% was weighted into the reactor and the MeOH: oil mole ratio of 6:1 was also added. The mixture was heated at 65°C and an agitation speed of 100 rpm was also set. After 1 h of reaction time, the product mixture was filtered to separate the

solid catalyst. The filtrate was poured into a separating funnel of 500 mL capacity for 12 h, to separate glycerol and unreacted methanol from the biodiesel. The remaining methanol in the recovered biodiesel was evaporated in an oven. The biodiesel yield was then determined using Equation 2:

Biodiesel yield (%) =
$$\frac{\text{Weight of biodiesel}}{\text{Weight of PKO}} X 100 (2)$$

F. Physico-chemical and GC-MS Analyses of the Biodiesel

Some fuel properties that determine the quality of biodiesel such as density, kinematic viscosity, flash point, cloud point, pour point, water and sulphur contents were evaluated for the PKB. The procedure described by[21] according to the ASTM D 6751 standard was used for the characterisations. The fatty acid methyl esters (FAMEs) in the PKB were also determined by an Agilent 7890A model of gas chromatography-mass spectroscopy (GC-MS). The procedure described by [24] was followed to carry out the investigation. The resulting spectra were compared to the standard in the NIST library (NIST 11).

III. Results and DiscussionA. Catalyst Characterisation

The FTIR spectra of the AMS, SSC800 and SSC900 were studied to figure out the absorption bands of the various materials in the samples as shown in Figure 1. For the AMS, a major spectrum at 1465 cm⁻¹ was observed which may be attributed to the asymmetric stretch of the CO₃²⁻ group.

The other two primary absorption bands found in the AMS spectra are 857 cm⁻¹ and 707 cm⁻¹ which can be assigned to out-of-plane and in-plane modes of vibration for the CO₃²⁻ molecules. The existence of these spectra in the AMS indicates the presence of

CaCO₃ which corroborates the findings in the literature [2], [15]. According to Figure 1, the SSC800 and SSC900 have similar spectra to the AMS. However, the calcination process at high temperatures of 800°C and 900°C resulted in the shifting of bands at higher energy.

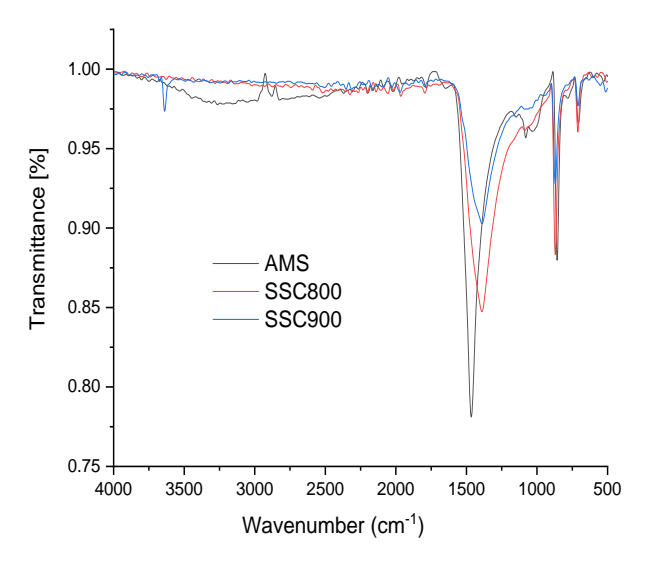
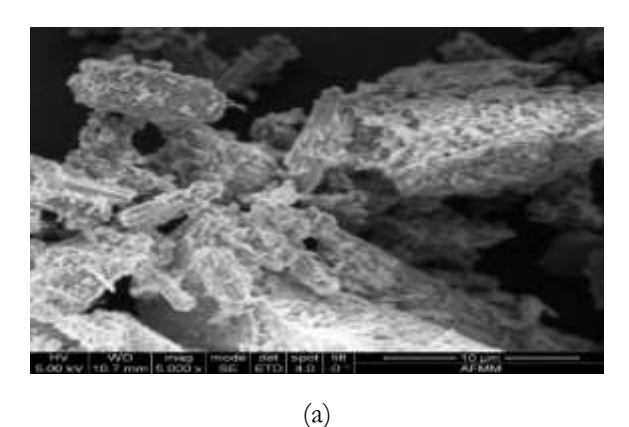


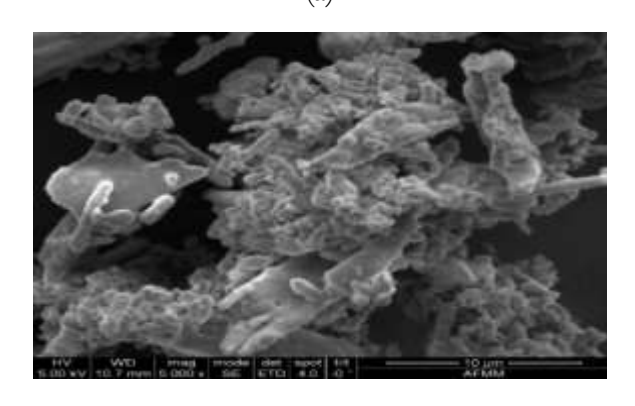
Figure 1: FTIR spectra of AMS, SSC800 and SSC900

This is due to the lower mass of the functional group connected to the CO₃²⁻ ion, which causes carbonate to be lost from the AMS [2]. Between 3674 and 3638 cm⁻¹, a sharp new peak appeared for SSC900 which may be as a result of the creation of basic -OH groups connected to the calcium atoms to give Ca(OH)₂[6]. It was also observed that the absorption band of the organic matter that appeared between 2879 and 2824 cm⁻¹ for the AMS disappeared after calcination, for the SSC800 and SSC900 catalysts. The FTIR also revealed that the band corresponding to CO₃²vanished after the calcination process of the AMS which confirms the breakdown of the CaCO₃ to CaO [15].

The surface morphology of AMS, SSC800 and SSC900 were carried out by the SEM as shown in Figure 2. The AMS (Fig. 2a) exhibited an amorphous structure of honeycomb surface with a particle size of

approximately between 2 and 4 µmwidth. The SEM micrograph as revealed by Figure 2a also shows significant agglomeration of the AMS. After calcination of the AMS, the SSC800 and





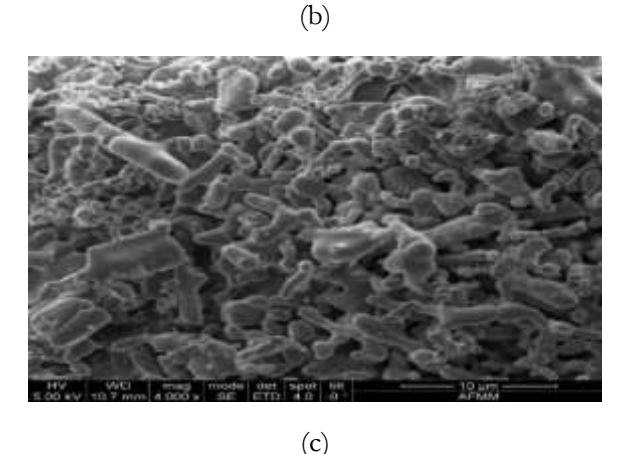


Figure 2: SEM of (a) AMS (b) SSC800 and (c) SSC900

SSC900 were formed and their SEM images are shown in Figures 2b and c respectively. The figures present rod-like regular shapes that are comparable to those described by Erchamo et al. [3]. Improved surface morphologies compared to that of the AMS were revealed by the figures, as large

porosities were observed. This demonstrates that the high calcination temperature resulted in a more porous structure in the samples [6]. This could be owing to the emission of water and gaseous CO₂. As CaCO₃ decomposes into CaO because the two substances act as porogens [15]. The width particle size of the SSC800 and SSC900 were also observed to be reduced to between 1 and 2 μm, an indication of improved surface area compared to the AMS.

Figure 3(a-c) presents the EDX of the samples which was investigated to determine elemental compositions before calcination for the AMS sample and after calcination for SSC800 and SSC900 samples. The major elements obtained in the samples were carbon, oxygen and calcium while silicon was only dominant in AMS and recessive in the other samples. The results revealed that the AMS contains 7.14% (w/w) of calcium, 37.97% (w/w) of carbon and 35.04% (w/w) of oxygen. While the SSC800 contains 22.60% (w/w) of calcium, 31.44% (w/w) of carbon and 43.20% (w/w) of oxygen and SSC900 contains 24.29% (w/w) of calcium, 35.30% (w/w) of carbon and 36.67% (w/w) of oxygen.

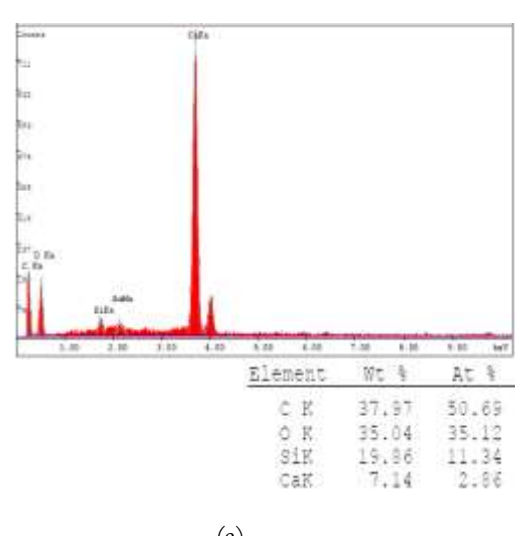
This shows that the conversion of the AMS to rich CaO catalysts of SSC800 and SSC900 is highly influenced by calcination at high temperatures of 800°C and 900°C respectively [2]. Also, the percentage composition of calcium increases with an increase in the calcination temperature, as seen in the figure. According to [15], this could be owing to the emission of CO₂ during the breakdown of CaCO₃ to CaO. It was also observed that the carbon content of the SSC900 slightly increased from 31.44% (w/w) to 35.30% (w/w) as a result of the increase in calcination temperature from 800°C to 900°C. This indicates that a further increase in temperature beyond 900°C could decrease the distribution

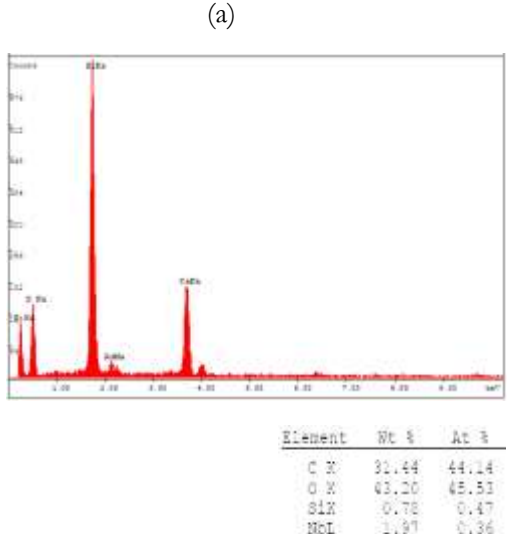
of calcium in the sample and increase the traces in the catalysts, its presence should not have negative impact any transesterification process. As it can mediate esterification of the TG's free fatty acid (FFA) content[3]. The result of the AAS shown in Table 4 further corroborates the findings in the EDX, as a similar pattern of percentage elemental contents was observed for each sample. The AAS result revealed that the elemental compositions prese (c) the catalysts are suitable transesterification of TG for biodiesel production. With each catalyst consisting of Ca, Mg, Na, Si and K in percentage proportion of 66.67, 1.12, 2.06, 3.01 and 9.33 for SSC800 respectively, while SSC900 consists of 59.33%, 1.03%, 2.30%, 2.50% and 8.00% respectively.

The BET surface area and pore volume of the AMS, SSC800 and SSC900 samples are revealed in Table 5. The table reveals that the surface area for AMS, SSC800 and SSC900 is 100.9 m²/g, 234.2 m²/g and 230.9 m²/g respectively, while those of the pore volume are 0.178 cc/g, 0.281 cc/g and 0.223 cc/g respectively. The values obtained revealed that the calcination process improved the surface area and pore volume of the SSC800 and SSC900 compared with those of the AMS.

However, the surface areas and pore volume for the SSC900 were lower than those of the SSC800 as a result of an increase in the calcination temperature from 800°C to 900°C. This might be due to the carbon deposit that occurred at the higher calcination temperature of 900°C as alluded in the EDX results. The sintering effect of extended heating at a higher temperature of 900°C is also responsible for the decrease in surface area for the SSC900 [15].

carbon content [6]. Though the silicon is in





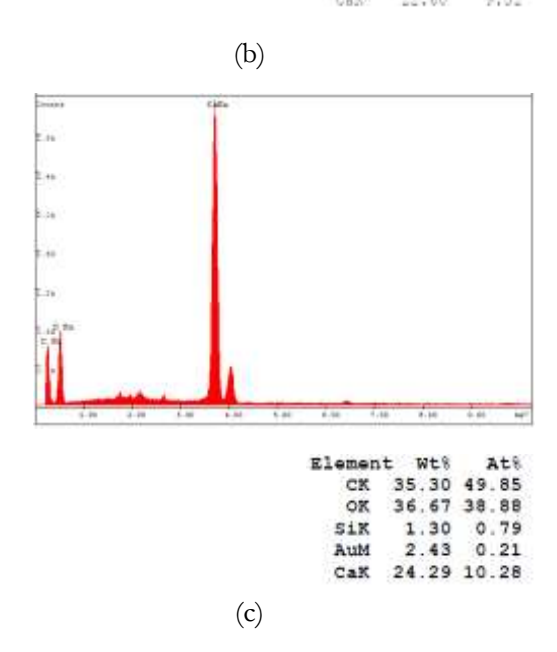


Figure 3: EDX of (a) AMS (b) SSC800 and (c) SSC900

Table 4: Elemental Composition of AMS, SSC800 and SSC900

Elements	AMS	SSC800	S900
	(%)	(%)	(%)
Calcium (Ca)	50.70	66.67	59.33
Magnesium (Mg)	22.00	1.12	1.03
Sodium (Na)	1.40	2.06	2.30
Silicon (Si)	9.30	3.01	2.50
Potassium (K)	1.05	9.33	8.00
Iron (Fe)	0.12	Trace	Trace
Zinc (Zn)	0.07	Trace	Trace
Copper (Cu)	0.01	Trace	Trace

Table 5: Size Analysis of Snail Shell Catalysts

Physical		AMS	SSC800	SSC900
Properti	es			
Surface	Area	100.9	244.2	230.9
(m^2/g)				
Pore	Volume	0.178	0.281	0.223
(cc/g)				
Pore Size	(nm)	1.324	1.324	1.324

The findings observed in the BET analysis further suggest that the calcination process has a significant effect on the surface area of the catalyst development. Hence, the SSC800 could have higher catalytic activity compared to the SSC900. As it has been reported that a catalyst's catalytic activity depends principally on its surface area, because the more the surface area, the more the catalytic activity [2]. Also, the pore volume increased during calcination of the AMS (0.178 cc/g) at a higher temperature of 800°C to form SSC800 (0.281 cc/g).Further increase calcination temperature to 900°C to produce SSC900 (0.223 cc/g) reduces the pore volume.

The growth of porosity after the calcination process of the AMS could describe the larger pore volume observed for the SSC800 and SSC900 catalysts. The production of pores in the catalyst was partially owing to the generation of CaO and partly due to the evolution of gaseous carbonisation products (CO₂ in this case) [15]. As a result, the presence of porosity on the surface of the SSC800 and SSC900 catalysts enhances the surface area and thus catalytic activity.

The basic strength distribution and basicity of the AMS, SSC800 and SSC900 samples were also evaluated and the results obtained are shown in Table 6. The AMS has a basic strength of $7.2 < H^- < 12.2$ while those of the SSC800 and SSC900 catalysts $7.2 < H^- < 18.4$ and $7.2 < H^- < 15.0$ respectively. The range obtained for the basic strength of the catalysts is higher than that of the AMS which is similar to the pattern of the surface area (Table 5). This supports the claim [15] that the basic strength of solid catalysts is directly proportional to their surface area. The basic strength obtained for the catalysts are high enough and can act as a strong base for transesterification reaction. More so that the CaO is a major constituent of the catalysts as shown in Table 4, their basic site is a very active species in the heterogeneous transesterification. The total basicity (basic site) was found to be 1.81 mmol/g, 4.33 mmol/g and 3.34 mmol/g for AMS, SSC800 and SSC900 respectively. The results show that the basic site of SSC800 was higher than those of the AMS and SSC900. This indicates that the calcination temperature of 800°C was sufficient to improve the basicity and surface area of the AMS to produce an SSC800 catalyst. Whereas, calcination temperature of 900°C reduces the basicity and surface area of SSC900 catalyst, which may be due to reduction in the CaO species (Table 4) in the catalyst [25]. This could mean that the SSC800 catalyst with higher basicity (number of basic sites) is expected to have higher catalyst activity [23].

B. Optimisation by DSD of the Transesterification of PKO using SSC800 and SSC900 Catalysts

Analysis of variance (ANOVA)

The optimisation study by a combination of different process conditions (Table 2) to optimise biodiesel yield based on the DSD

Table 6: Basic Strength and Basicity of the Samples

Sample	Basic strength range	Basicity (mmol/g)		
		Weak	Medium	Total
		basic	basic	
		sites	sites	
AMS	7.2< <i>H</i> ⁻ <12.2	1.56	0.25	1.81
SSC800	7.2< <i>H</i> ⁻ <18.4	2.80	1.53	4.33
SSC900	7.2< <i>H</i> ⁻ <15.0	2.01	1.33	3.34

was investigated. The complete experimental matrix and actual biodiesel yield for 18 experimental runs as obtained from the DSD are shown in Table 7. The data of the experimental matrix and actual biodiesel yield were put through sophisticated multiple regression analysis. This was done to get a polynomial second-order equation regression coefficients that could be used to test for statistical significance. The regressors model F-value of 166.6725 with a p-value of 0.0001 revealed that the model is highly significant at a 95% confidence level, based on the ANOVA findings provided in Table 8. This means that the regression model accurately forecasts biodiesel yield. From Table 8, process conditions of MeOH: oil mole ratio, temperature, catalyst quantity and catalyst calcination temperature have p-values <<0.05. This indicates that aforementioned process conditions are highly significant to influence biodiesel yield. Also, by comparing the actual and predicted results with tolerable accuracy of the model through the statistical approach of data fitting, coefficient of regression (R²) and adjusted coefficient of regression (Adj-R²) indicate the model's dependability.

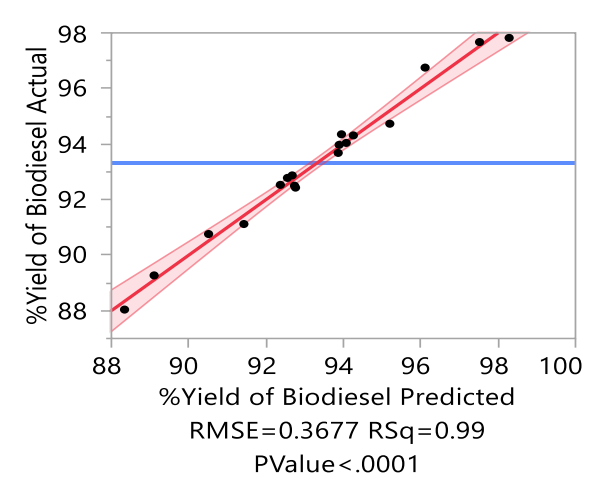


Figure 4: Plot of experimental versus predicted values of %yield of the biodiesel

As shown in the table, values of R² (0.9858) and Adj-R² (0.9799) suggests that 98.58% and 97.99% of the total disparity in the biodiesel yield is ascribed to the independent variables investigated. These results reveal that the actual and predicted values are in good agreement, since the R² value is close to unity (1.0), implying that the empirical models closely match the experimental data [14]. Figure 4 depicts the consistency of actual (y-axis) values and predicted (x-axis) values in a plot, which are comparable to a line of unit slope (45°). The data are also extremely close to the line of the perfect fit, indicating a good agreement between the actual and predicted data.

Furthermore, from among the models (linear, two-factor interaction (2FI) and quadratic) that exist in the software, the linear model was suggested to analyse Eq. (1) to obtain the solution of Equation 3:

$$Y = 92.26 - 0.40X_1 - 0.88X_2 + 0.85X_3 - 0.23X_4 + 2.39X_5$$
 (3)

Where; $X_1 = \text{MeOH}$: oil mole ratio (w/w), $X_2 = \text{Temperature (C)}$, $X_3 = \text{Catalyst quantity } (w/w)$, $X_4 = \text{Reaction time (h)}$ and $X_5 = \text{Catalyst calcination temperature (C)}$.

Table 7: Experimental Matrix for the Process Conditions and Response for the DSD

Exp. Runs	MeOH: Oil Mole Ratio (w/w)	Temperature (°C)	Catalyst Quantity (%, w/w)	Reaction Time (h)	Catalyst Calcined Temperature (°C)	%Yield of biodiesel
1	6	65	4	1	800	92.78
2	8	60	4	2	800	97.97
3	10	65	2	1	900	87.13
4	6	55	6	1	900	93.53
5	8	60	4	2	900	91.50
6	8	55	2	1	800	97.67
7	10	55	4	3	900	98.04
8	10	65	2	3	800	96.31
9	8	65	6	3	900	98.27
10	6	55	6	3	800	93.68
11	10	55	6	1	800	81.87
12	6	65	6	2	800	86.76
13	6	55	2	3	800	97.82
14	6	60	2	1	900	94.73
15	10	60	6	3	800	91.12
16	6	65	2	3	900	84.35
17	10	55	2	2	900	83.75
18	10	65	6	1	900	88.04

Table 8: ANOVA and statistical values estimated for the process conditions

Source		Sum c	of DF	Standard	t Ratio	F Ratio	Prob> t
		Squares		Error			(p-value)
Model		112.67071	5	0.0973	958.62	166.6725	<.0001
MeOH: oil mole Temperature (%)		2.474436 34.820472	1 1	0.0991 0.0991	-4.28 -16.05	18.3020 257.5476	0.0011 <.0001
Catalyst quantit	ty (%, w/w)	67.257668	1	0.0991	-22.30	497.4675	<.0001
Reaction time (h)	0.399672	1	0.0991	1.72	2.9562	0.1112*
Catalyst calcina	tion	5.617838	1	0.089556	6.45	41.5520	<.0001
temperature [80	00]						
Residual		1.62240	12				
R ²	R ² Adj		Mean re Error	Mear	n of Respon	se Observa Sum Wg	(-

^{*}Insignificant

0.985805

The analysis of the model was to further establish the process conditions that have significant effects on the biodiesel yield based on coded parameters. The equation suggests that the 2FI and quadratic factors are

0.97989

insignificant in the process, hence their nonappearance in the equation. The significant factors with positive signs in the equation also suggest a synergistic effect that greatly influences the linear terms to boost biodiesel

18

93.31222

0.367696

Source	Log Worth	p-value
Catalyst Quantity (w/w) (2, 6)	10.410	0.00000
Temperature (°C) (55, 65)	8.747	0.00000
Calcination temperature (°C) (800,900)	4.498	0.00003
MeOH: oil mole ratio (w/w) (6, 10)	2.970	0.00107
Reaction time (h) (1, 3)	0.954	0.11121

Figure 5: Rate of contributing effect of each process parameters on biodiesel yield

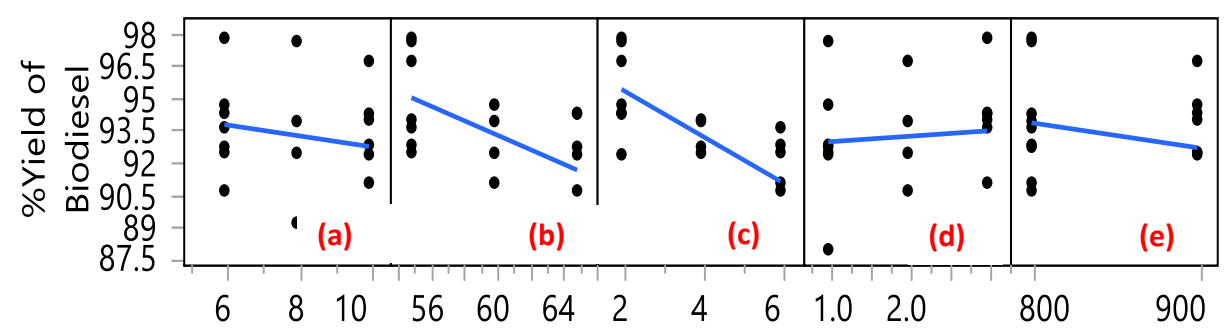


Figure 6: Plots of Linear Effect of Process Parameter (a) MeOH: oil mole ratio, (b) Temperature, (c) Catalyst quantity, (d) Reaction time and (e) Calcination temperature on %Yield of Biodiesel

yield. Negative signs indicate that the linear parameters have an antagonistic effect on biodiesel yield. Figure 5 shows the rate at which each of the process conditions contributes to significantly influencing the biodiesel yield.

The figure shows that the catalyst quantity with the highest LogWorth of 10.410 has the most influence among the process conditions on the biodiesel yield, followed by the temperature with LogWorth of 8.747. The calcination temperature with LogWorth of 4.498 is the next significant process condition after temperature, followed by MeOH: oil mole ratio (LogWorth = 2.970).

The least significant of the process conditions is reaction time with LogWorth of 0.954. These findings reveal the order in which each process condition influence the biodiesel yield of the PKO.

C. Linear Effects of the Process Conditions on the Biodiesel Yield

Figure 6a shows the effect of a MeOH: oil mole ratio ranging from 6:1 to 10:1 on biodiesel output. As the MeOH: oil mole ratio

increases from 6:1 to 10:1, the average biodiesel yield declines from 94% to 92.7

This means that the highest biodiesel yield came from a MeOH: oil mole ratio of 6:1, which was higher than the stoichiometrically established value (more than 3:1). This implies that a 6:1 mole ratio of MeOH to oil is enough to move the reaction equilibrium towards the end products. However, the excess mole ratio of MeOH: oil beyond 6:1 resulted in the decrease of the conversion due to the formation of a relatively complicated reaction mixture. As the excess of methanol could limit the contact between TG and active sites in the catalyst, thereby creating diffusion restrictions[26].

The effect of reaction temperature ranging between 55°C and 65°C on the %yield of biodiesel from PKO is shown in Figure 6b. It was discovered that a temperature of 55°C resulted in a better biodiesel yield of 95% and at a higher temperature of 65°C, the %yield drops to 92%. According to [27], an increase in the reaction temperature supposed to enhance the kinetic energy by boosting the collision between molecules in the reaction

mixture, thereby increasing the biodiesel yield. However, temperatures above 55°C resulted in decreased biodiesel yields due to methanol vapourisation into the gas phase, which causes reduced interaction with the PKO [28]. The higher temperature could also have favoured saponification reaction and lowered the biodiesel yield [12].

Effect of catalyst quantities of 2, 4 and 6 (%, w/w) on the biodiesel production from PKO to biodiesel was studied, with the result given in Figure 6c. It was observed that the average biodiesel yield of 95%, 93.5% and 91.5% was obtained at catalyst quantity of 2% (w/w), 4% (w/w) and 6% (w/w) respectively. This demonstrates that a catalyst quantity of 2% vielded the greatest biodiesel (w/w)production of 95%. This indicates that the 2% (w/w) catalyst's active sites were capable of completing the reaction for optimum biodiesel yield. As a result, higher catalyst concentration beyond 2% (w/w) might well have raised the viscosity of the reaction composition and lowered the process's mass transfer efficiency [27]. Excess catalyst quantity in the reaction mixture may have also led to soap formation, instead of biodiesel production and consequently reduce the biodiesel yield [12].

To get the best biodiesel production, the reaction must be allowed to achieve equilibrium and there must be adequate contact time between the reactants and catalysts. Therefore, the influence of reaction time of 1 h and 3 h on the per cent yield of biodiesel from PKO was studied and shown in Figure 6d. It was revealed that the biodiesel yield of 93%, 93.5% and 94% were obtained at 1 h, 2 h and 3 h respectively.

This supports the ANOVA result in Table 8, which shows that the influence of time of reaction on biodiesel yield is negligible. Because a prolonged reaction time can cause the CaO in the catalyst to absorb the biodiesel, thereby lowering the yield [11]. As a result, 1 h of reaction time is adequate for the catalyst to reach equilibrium and produce the best biodiesel yield.

Effect of calcination temperatures of 800°C and 900°C on the efficiency of the catalyst for biodiesel production using PKO undertaken and the result obtained is shown in Figure 6e. From the figure, 800°C that produced SSC800 catalyst revealed a better average biodiesel yield of 94% than SSC900 catalyst of 900°C which yielded 92.5%. This shows that the temperature of 800°C was the most suitable temperature for the development of the catalyst (SSC800) from the AMS. The SSC800 catalyst's superior performance can be due to the increased surface area provided by a high calcination temperature of 800°C. This further supports the claim of [12] that the temperature at which solid catalysts are produced is critical to their activity. As the calcination temperature is responsible for the generation of the active site of mixed oxides as well as the destruction of organic materials in the AMS.

D. Effects of Interaction Between Process Conditions on the Biodiesel Yield

The interactive influence of process conditions on the %yield of biodiesel was studied by plotting contours in two dimensions (2D) graphs as shown in Figure 7

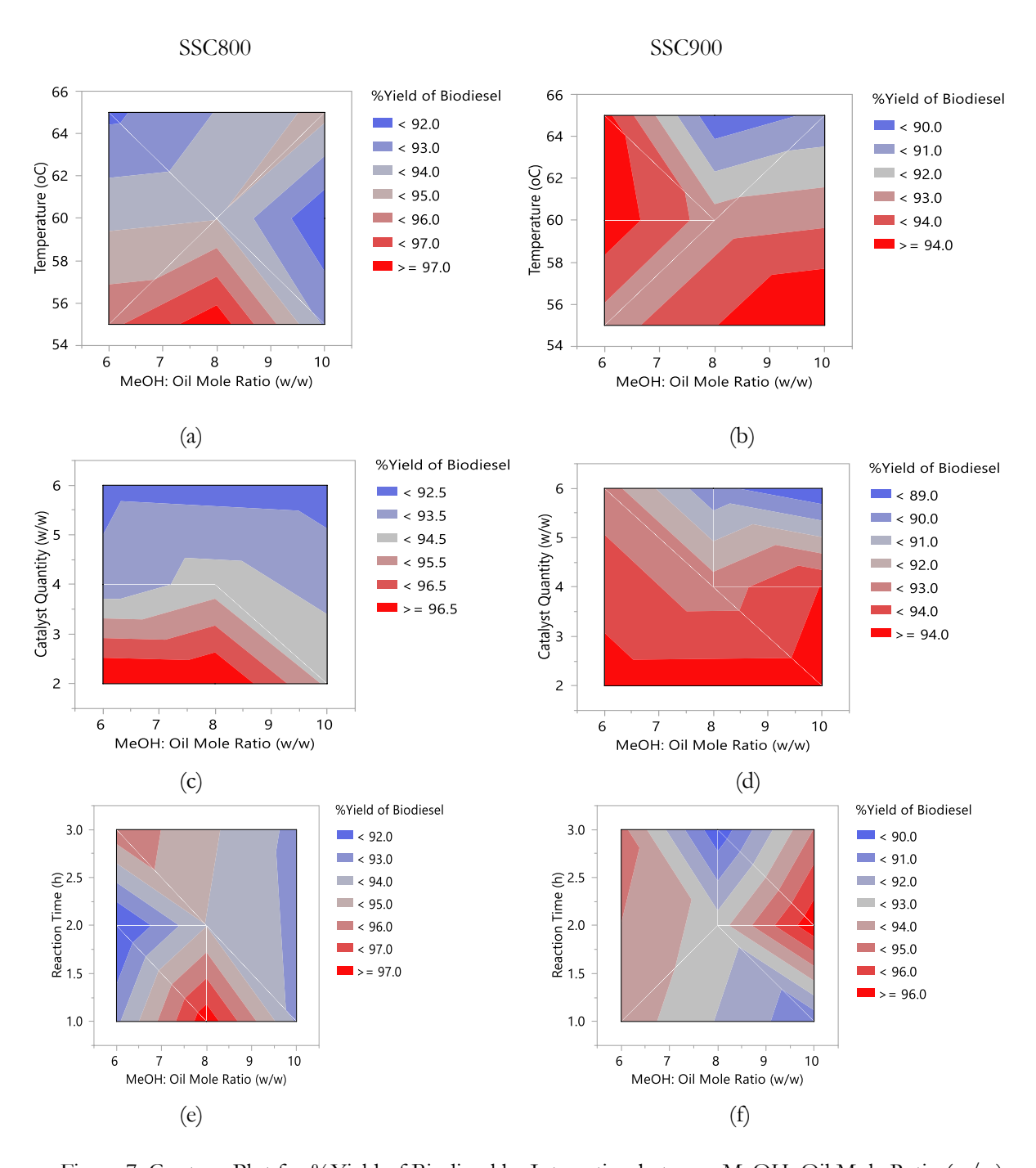


Figure 7: Contour Plot for %Yield of Biodiesel by Interaction between MeOH: Oil Mole Ratio (w/w) and Other Parameters for SSC800 and SSC900

. The 2D plots are the graphical depiction of the biodiesel production achieved from the experimental runs in terms of the various process conditions. Figure 7 (a and b) depicts the combination influence of MeOH: oil mole ratio and temperature on biodiesel yield for SSC800 and SSC900 respectively. When the SSC800 catalyst was used, the biodiesel

production increases to 97% with a rise in excess mole ratio of MEOH: oil to 8:1 at a temperature of 50°C. While the biodiesel yield drops to 92% when the excess MEOH: oil mole ratio was increased to 10:1.

This corroborates the findings of [29] who found that increasing MeOH can reduce biodiesel yield by increasing the concentration

of glycerol in the reaction composition. As a result, the equilibrium would shift to the reactant side of the reaction, thus lowering the yield of biodiesel. However, because transesterification is a reversible process in nature, a large amount of MeOH is necessary to keep the chemical reaction moving forward.

The effect of the interaction between the mole of MeOH: ratio oil and the catalyst concentration of SSC800 and SSC900 on biodiesel yield is shown in Figure 7 (c and d). Figure 7c revealed that when the mole ratio of methanol to oil was in the range of 6:1 to 8:1 at a low catalyst quantity of 2% (w/w) for SSC800 catalyst, the yield of biodiesel increased to >=96.5%. While Figure 7d showed the highest biodiesel yield >=96.5% when methanol to oil mole ratio was in the range of 6:1 to 10:1 at a low catalyst concentration of 2% (w/w) for SSC900 depicted catalyst. This that the concentration of both catalysts (SSC800 and SSC900) rose with the molar ratio, the biodiesel yield decreased. This could be because of the development of emulsion which makes biodiesel phase separation challenging and as such reduces the yield [14].

Figures 7 (e and f) reveal the interactive effect between methanol: oil mole ratio and rate of reaction on biodiesel yield at SSC800 and SSC900 catalysts respectively. The production rate of biodiesel increases to ≥97% yield when the MeOH: oil mole ratio increases to 8:1 at an idea reaction time of 1 h for the reaction in the presence of SSC800 catalyst (Figure 7e). Beyond the mole ratio of 8:1 and rate of reaction above 1 h, the yield of biodiesel decreases to <96% for the catalyst. This supports the claim of[30] that the excess MeOH in the reaction over a longer reaction period increases the solubility of the glycerol,

thereby triggering a reverse reaction and lowering the biodiesel yield. From Figure 7f, the SSC900 catalyst behaves differently, as a higher MeOH: oil mole ratio of 10:1 and a reaction time of 2 h gave the highest biodiesel yield of ≥96%. This shows that the high MeOH: oil molar ratio reduces the critical temperature and enables high biodiesel yield. As the excess MeOH drives the equilibrium to the product side and a longer reaction time induces a high rate of reaction, thus successively increasing the biodiesel yield for the SSC900 catalyst [31].

Figures 8 (a and b) reveal the influence of reaction temperature and catalyst quantity on the yield of biodiesel using SSC800 and SSC900 catalysts respectively. The 2D figure for the SSC800 catalyst (Figure 8a) presented an optimum ≥97% biodiesel yield under a lower temperature of 55°C and a lower catalyst amount of 2% (w/w). This shows that the interactive effect of reaction temperature and catalyst quantity on the yield of biodiesel is negative. A lower catalyst quantity with a decrease in the reaction temperature greatly enhanced the yield of biodiesel from PKO the SSC800 catalyst was Therefore, the reaction temperature >55°C and catalyst quantity >2% (w/w) were established to step-wisely decline the biodiesel vield to <92%. This is because a higher catalyst quantity combined with a rising reaction temperature would elevate the risk of saponification by converting the TG to soaps, thus, reducing the biodiesel yield [32, 33]. Figure 8b shows similar patterns for the SSC900 catalyst, which yielded ≥96% biodiesel at a process temperature of 55°C and a catalyst amount of 2% (w/w). This indicates that both the SSC800 and SSC900 catalysts behave likewise under the same conditions of process temperature and catalyst amount during transesterification reaction.

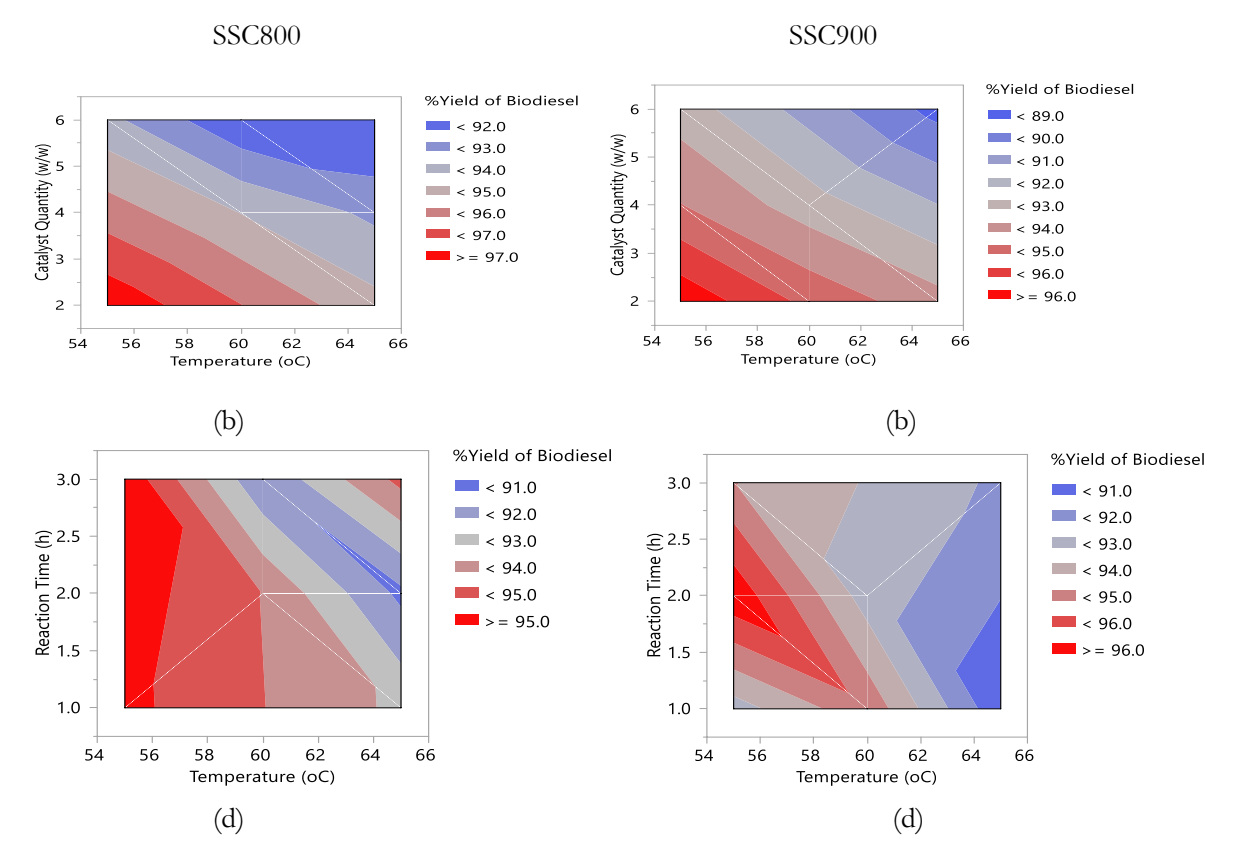


Figure 8: Contour Plot for %yield of Biodiesel by Interaction between Temperature (°C) and Other Parameters for SSC800 and SSC900

The influence of process temperature and reaction duration on biodiesel yield by the SSC800 and SSC900 catalysts is shown in Figures 8 (c and d). The plot shows that increasing the process temperature while increasing the reaction time does not result in a higher yield of biodiesel. For the SSC800 catalyst, an optimum biodiesel yield of 95% was recorded at 55°C and a reaction time of 1 h to 3 h (Figure 8c).

Hence, an increase in temperature from 55°C to 65°C reduces the biodiesel drastically to <91% yield, even at any given reaction duration of between 1 h and 3 h. This is because the saponification of TG by CaO catalyst is enhanced at a temperature >50°C [32]. From Figure 8d, an optimum biodiesel yield of ≥96% was achieved at 55°C temperature and a reaction period of 2 h for SSC900 catalyst. This shows that the catalyst is more sensitive to change in reaction time as the yield decreases at a low reaction period (1 h) and a higher reaction time (3 h). This is because the extended reaction duration could cause esters to hydrolysed, causing additional

fatty acids to produce soap [20]. It is however impossible to achieve a higher yield of biodiesel when the reaction time is more or less than 2 h for this catalyst, irrespective of the reaction temperature [34]. Therefore, ultimate conversion efficiency of 98.29% was achieved for the biodiesel production under methanol: oil mole ratio of 6:1, process temperature of 55°C, catalyst amount of 2% (w/w), reaction duration of 3 h, and catalyst calcination temperature of 800°C (SSC800 catalyst) as presented in Table 9.

E. Empirical Verification of Optimal Parameters for Biodiesel Yield

Optimisation of process parameters of methanol: oil mole ratio, 6:1, process temperature, 55°C, catalyst amount, 2% (w/w), reaction duration, 3 h and catalyst calcination temperature, 800°C (SSC800 catalyst) was performed using the empirical approach to validate the predicted maximum biodiesel yield given by the DSD.

The consistency of the predicted result for biodiesel yield was confirmed by repeating the experiment in triplicate using the attained optimal operating parameters as presented in Table 9.

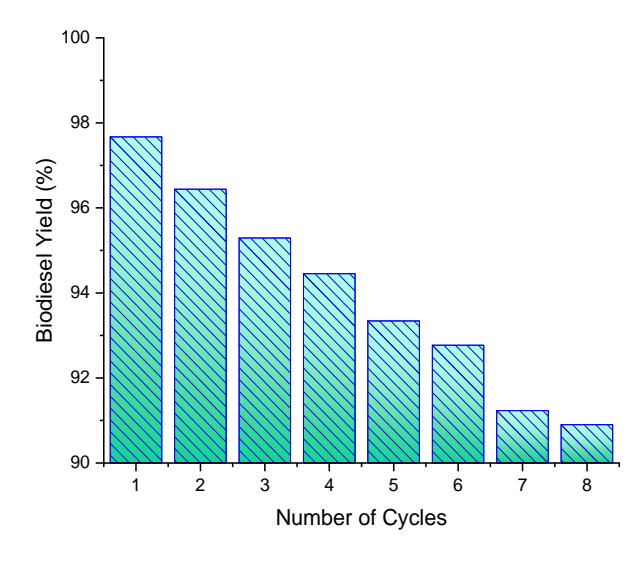


Figure 9: Recyclability study of SSC800 catalyst at optimal

The average yield of biodiesel achieved for the validation study was 98.40% with a percentage error of 0.49% when related to the predicted result of 98.29%. The %error obtained was <0.5% which shows a good relationship between the predicted and experimental results. It can be resolved that the DSD was a perfect tool to predict the optimisation process for PKO to biodiesel using the SSC800 and SSC900 catalysts.

F. Reusability Study of SSC800 Catalyst for Biodiesel Production using PKO

One of the benefits of heterogeneous catalysts over homogeneous catalysts is their ease of recovery and reusability over lengthy periods [35]. The reusability of solid catalysts is also one of the most important factors to consider when evaluating their stability and economic viability for biodiesel production in a

commercial scale[20]. As a result, this study explores the reusability of the best functioning catalyst (SSC800) under 6:1 methanol: oil mole ratio, 55°C process temperature, 2% (w/w) catalyst amount, and 3 h reaction period. As shown in Figure transesterification process was carried out over 8 cycles and revealed that the catalytic activity gradually decreases with increase in number of cycles. The figure showed that the biodiesel yield was 98.40% at first run and reduced to 94.45% after 4th cycle and further declined to 90.9% at 8th cycle. Though the reduction in the biodiesel yield over the cycles is minimal, the decrease is a result of a decrease in the surface area, pore volume and total basicity of the catalyst. The reduction in the biodiesel yield over the cycles was also attributable to adsorption-induced leaching and aggregated poisoning of active sites. Due to the leaching of active components (Ca²⁺) from the SSC800 catalyst, the availability of active sites will steadily decrease with repeated usage of the catalyst [14]. Therefore, it can be concluded from the investigation that the SSC800 catalyst can be repeatedly used over 7 cycles with <5% loss in the biodiesel yield.

G. Physicochemical Characteristics of the Biodiesel

The quality of the produced PKB using the SSC800 catalyst was evaluated under key physical properties as shown in Table 10. The obtained fuel properties for the PKB were compared with the ASTM standard for diesel and biodiesel as presented by [21]. The table shows that all the properties measured are within the prescribed limit of the biodiesel ASTM standards. The density of the PKB (0.866 g/cm³) is inconsequentially above the diesel standard (0.860g/cm³), which could be due to the fatty acid composition and purity [31].

Table 9: Optimal Conditions for %Yield of PKB

Optimal process conditions	\mathbf{X}_1	\mathbf{X}_2	X_3	X_4	X_5	%PKB	PKB LCI	PKB UCI
Predicted	6	55	2	3	800	98.29	97.80	98.77
Experiment 1						97.88		
Experiment 2						99.01		
Experiment 3						98.30		
Average biodiesel yield						98.40		

LCI = Lower Confidence Interval, $X_1 = MeOH$: Oil Mole Ratio (w/w), (w/w), $X_4 = Reaction Time$ (hours), UCI = Upper Confidence Interval,

PKB = Biodiesel

 X_2 = Reaction Temperature (°C),

 $X_3 = Catalyst Quantity$

%PKB

(w/w), X_4 = Reaction Time (hours), X_5 = Catalyst Calcination Temperature (°C), %Yield of Biodiesel

Table 10: Fuel Properties of the PKB, the ASTM Standard for Diesel and Biodiesel

Fuel properties (units)	PKB	Biodiesel standard	Diesel standard
		ASTM D 6751	ASTM D 975
Density@15°C(g/cm³)	0.866	0.860 - 0.900	0.800 - 0.860
Kinematic viscosity@40°C (mm ² /s)	2.9	1.9 - 6.0	1.3 - 4.1
Flash point (°C)	129	100 - 170	60 - 80
Cloud point (°C)	10	-3 - 15	-35 - 5
Pour point (°C)	8	-5 - 10	-35 to -15
Water content (%, v/v oil)	< 0.005	≤ 0.05	-
Sulfur content (%, v/v oil)	< 0.005	≤ 0.005	-
Source	This study	Birla et al. (2012)	

However, the density falls within the range of the biodiesel standard (0.860 – 0.900 g/cm³). Krishnamurthy et al. [14] elucidated the significance of the kinematic viscosity of biodiesel as it affects its performance in diesel engines. It was reported that the higher kinematic viscosity of biodiesel disturbs fuel spray atomization, spray penetration, flowability and more difficulties in cold weather.

Worthy of note is that the kinematic viscosity obtained for the PKB (2.9 mm²/s) falls within the range of biodiesel standard (1.9 – 6.0 mm²/s) and even that of the diesel standard (1.3 – 4.1 mm²/s). The flashpoint of the PKB (129°C) was found to be well within the specified range of biodiesel standard (100 – 170°C). However, the obtained value for PKB was higher compared with the diesel standard (60 – 80°C), which implies that the biodiesel is less volatile and easy for transportation and storage [31]. The cloud and pour points of

PKB was 10°C and 8°C respectively, which falls within the standard of biodiesel (-3 – 15°C and -5 – 10°C) and diesel standard (-35 – 5°C and -35 to 15°C). The results revealed that the PKB is a suitable fuel for cold weather regions without causing fuel injector problems, deposit formation, poor fuel atomization and incomplete combustion [36].

The water content of the PKB was <0.005(%, v/v oil), which indicates that the biodiesel would not degrade and cause the formation of whitish sediments that can clog filters and restrict fuel flow to the engine [37]. The sulphur content of the PKB was also <0.005(%, v/v oil) which is within the limit of the standard. The GC-MS analysis reveals about eight main characteristic peaks of FAMEs appearing at different retention times as shown in Table 11. The chemical and percentage compositions of each of the peaks are also shown in the table with methyl laurate(35.06%) as the highest concentration

followed by methyl oleate (24.72%), methyl myristate (15.84%) and methyl palmitate (11.22%).

Table 11: FAMEs profile of PKB

Pea	Retenti	FAME	Molecul	0/0
k	on time	s	ar	composi
no.	(min)	present	formula	tion
1	14.78	Methyl	C ₉ H ₁₈ O ₂	0.73
		caprylo		
		ate		
2	21.92	Methyl	$C_{11}H_{22}O_2$	2.54
		caprate		
3	26.86	Methyl	$C_{12}H_{24}O_2$	35.06
		laurate		
4	31.06	Methyl	$C_{14}H_{28}O_2$	15.84
		myristat		
		e		
5	34.13	Methyl	$C_{16}H_{32}O_2$	11.22
		palmitat		
		e		
6	37.90	Methyl	Methyl $C_{19}H_{38}O_2$	
		stearate		
7	38.30	Methyl C ₁₈ H ₃₄ O ₂		24.72*
		oleate		
8	-	Others	-	4.08

*The unsaturated fatty acid methyl ester

Other FAMEs present in the PKB, though in relatively smaller amounts are methyl caprate (2.54%), methyl stearate (2.29%) and methyl capryloate (0.73%). All the FAMEs identified in the PKB are saturated types except methyl oleate which is unsaturated FAME.

This indicates that the PKB contains more saturated FAME which is an important characteristic in biodiesel. Usually, the more the presence of the saturated FAME, the more the cetane contribution and stability of the biodiesel [38]. Therefore, the physical and chemical properties obtained for the biodiesel from PKO is feasible as an environmentally friendly and alternative fuel to petro-diesel.

IV. Conclusion

The heterogeneous catalysts of SSC800 and SSC900 developed from the calcination of *ArchachatinaMarginata*snailshell at 800°C and 900°C, respectively, were found suitable for

the transesterification of palm kernel oil. It was established that the catalysts contained essential ingredients such as Ca, Mg, Na, Si and K in great proportion suitable for biodiesel production. The characterisation investigations confirmed that the SSC800 should perform better than the SSC900 due to their surface area, which was corroborated by the optimisation study. The process conditions that gave optimum biodiesel yield of 98.28% with the SSC800 catalyst are MeOH: oil molar ratio of 6:1, the reaction time of 3 h, the temperature of 55°C and catalyst quantity of 2% (w/w). The quality of the PKB was confirmed by comparing its physicochemical properties with the ASTM standard of biodiesel. Therefore, this study utilised cost-effective and environmentfriendly Archachatina marginata snail-shell for catalysts development to produce quality biodiesel from PKO.

References

- [1] Oyelaran, O.A., Bolaji, B.O. and Mansur, O. "Preparation and Characterization of Calcium Oxide Heterogeneous Catalyst Derived from Guinea Fowl Egg Shell for Biodiesel Synthesis for a Sustainable Future", *Int. J. Innov. Res. Educ. Technol. Soc. Strateg.*, vol. 6, no. 1, 2019, pp. 134–148.
- [2] Niju, S., Anushya, C. and Balajii, M. "Process Optimization for Biodiesel Production from Moringa oleifera Oil Using Conch Shells as Heterogeneous Catalyst", *Environ. Prog. Sustain. Energy*, 2018, pp. 1–12.
- [3] Erchamo, Y.S., Mamo, T.T. and Workneh, G.A. "Improved Biodiesel Production from Waste Cooking Oil with Mixed Methanol ethanol using Enhanced Eggshell-derived CaO nano-catalyst", *Sci. Rep.*, 2021, pp. 1–12.
- [4] Ajala, E.O., Ajala, M.A., Ajao, A.O., Saka, H.B. and Oladipo, A.C. "Calcium-Carbide Residue: A Precursor for the Synthesis of CaO–Al₂O₃–SiO₂–CaSO₄ Solid Acid Catalyst for Biodiesel Production using Waste Lard", *Chem.*

- Eng. J. Adv., vol. 4, no. August, 2020a.
- [5] Ajala, E.O., Ajala, M.A., Odetoye, T.E. and Okunlola, A.T. "Synthesis of Solid Catalyst from Dolomite for Biodiesel Production using Palm Kernel Oil in an Optimisation Process by Definitive Screening Design", *Brazilian J. Chem. Eng.*, vol. 36, no. 02, 2019a, pp. 979–994.
- [6] Hazri, M.M. and Nasir, N.F. "Calcium Oxide from Waste Shells as Potential Green Catalyst for Biodiesel Production", Res. Prog. Mech. Manuf. Eng., vol. 1, 2020, pp. 44–55.
- [7] Ajala, E.O., Ajala, M.A., Okedere, O.B., Aberuagba, F. and Awoyemi, V. "Synthesis of Solid Catalyst from Natural Calcite for Biodiesel Production: Case Study of Palm kernel Oil in an Optimisation Study using Definitive Screening Design", *Biofuels*, 2019b, pp. 1–12.
- [8] Kaewdaeng, S., Sintuya, P. and Nirunsin, R. "Biodiesel Production using Calcium Oxide from River Snailshell Ash as Catalyst", *Energy Procedia*, vol. 138, 2017, pp. 937–942.
- [9] Ugbede, A.C., Jumoke, E.E. and Abdullahi, M.A. "Development and Application of Heterogeneous Catalyst from Snail Shells for Optimization of Biodiesel Production from Moringa *Oleifera* Seed Oil", *Am. J. Chem. Eng.*, vol. 9, no. 1, 2021, pp. 1–17.
- [10] Kaewdaeng, S. and Nirunsin, R. "Synthesis of Calcium Oxide from River Snailshell as a Catalyst in Production of Biodiesel", *Appl. Environ. Res.*, vol. 41, no. 1, 2019, pp. 31–37.
- [11] Trisupakitti, S. Ketwong, C., Senajuk, W., Phukapak, C. and Wiriyaumpaiwong, S. "Golden Apple Cherry Snail Shell as Catalyst for the Heterogenous Transesterification of Biodiesel", *Brazilian J. Chem. Eng.*, vol. 35, no. 04, 2018, pp. 1283–1291.
- [12] Ajala, E.O., Ajala, M.A., Odetoye, T. E., Aderibigbe, F.A., Osanyinpeju, O.H. and Ayanshola, M.A. "Thermal Modification of Chicken Eggshell as Heterogeneous Catalyst for Palm Kernel Biodiesel Production in an Optimisation Process", *Biomass Convers. Biorefinery*, 2020b, pp. 1–19.

- [13] Odetoye, T.E., Agu, J.O. and Ajala, E.O. "Biodiesel Production from Poultry Wastes: Waste Chicken Fat and Eggshell", *J. Environ. Chem. Eng.*, vol. 9, no 4, 2021, pp. 1-8.
- [14] Krishnamurthy, K.N., Sridhara, S.N. and Kumar, C.S.A. "Optimisation and Kinetic Study of Biodiesel Production from *Hydnocarpus wightiana* Oil and Dairy Waste Scum using Snail Shell CaO Nano Catalyst," *Renew. Energy*, vol. 146, 2020, pp. 280–296.
- [15] Laskar, I.B., Rajkumari, K., Gupta, R., Chatterjee, S., Paul, B. and Rokhum, L. "Waste Snail Shell Derived Heterogeneous Catalyst for Biodiesel Production by the Transesterification of Soybean Oil", R. Soc. Chem. Adv., vol. 8, 2018, pp. 20131–20142.
- [16] Saha, C., Pramanik, S., Chakraborty, J., Parveen, S. and Aditya, G. "Abundance and Body Size of the Invasive Snail Physa Acuta Occurring in Burdwan, West Bengal, India," *J. Entomol. Zool. Stud.*, vol. 4, no. 4, 2016, pp. 490–497.
- [17] Ademolu, K.O., Akintola, M.Y., Olalonye, A.O. and Adelabu, B.A. "Traditional Utilisation and Biochemical Composition of Six *Molluse* Shells in Nigeria," *Int. J. Trop. Biol.*, vol. 63, no. 2, 2015, pp. 459–464.
- [18] Akinnusi, F.A.O., Oni, O.O. and Ademolu, K.O. "Mineral Composition of Giant African Land Snail's (*Archachatina marginata*) Shells from Six South West States, Nigeria", *Niger. J. Anim. Sci.*, vol. 20, no. 4, 2018, pp. 485–489.
- [19] Otori, A.A., Mann, A., Suleiman, M.A.T. and Egwim, E.C. "Synthesis of Heterogeneous Catalyst from Waste Snail Shells for Biodiesel Production using *Afzelia* Africana Seed Oil," *Niger. J. Chem. Res.*, vol. 23, no. 1, 2018, pp. 35–51.
- [20] Gupta, J. and Agarwal, M. "Preparation and Characterisation of Highly Active Solid Base Catalyst from Snailshell for Biodiesel Production", *Biofuels*, vol. 7269, 2016, pp. 1–10.
- [21] Birla, A., Singh, B., Upadhyay, S. N. and Sharma, Y.C. "Kinetics Studies of Synthesis of Biodiesel from Waste Frying Oil using a Heterogeneous Catalyst Derived from Snail Shell,"

- Bioresour. Technol., vol. 106, 2012, pp. 95-100.
- [22] Liu, H., Guo, H., Wang, X., Jiang, J., Lin, H. and Han, S. "Mixed and Ground KBr-Impregnated Calcined Snail Shell and Kaolin as Solid Base Catalysts for Biodiesel Production", *Renew. Energy*, vol. 93, 2016, pp. 648–657.
- [23] Zeng, H.Y., Xu, S., Liao, M.C., Zhang, Z.Q. and Zhao, C. "Activation of Reconstructed Mg/Al Hydrotalcites in the Transesterification of Microalgae Oil", *Appl. Clay Sci.*, vol. 91–92, 2014, pp. 16–24.
- [24] Ajala, E.O., Aberuagba, F., Olaniyan, A.M., Ajala, M.A. and Sunmonu, M.O. "Optimisation of a Two-stage Process for Biodiesel Production from Shea Butter using Response Surface Methodology", *Egypt. J. Pet.*, vol. 26, no. 4, 2017, pp. 943-955.
- [25] Ooi, H.K., Koh, X.N., Ong, H.C., Lee, H.V., Mastuli, M.S., Taufiq-Yap, Y.H., Alharthi, F.A., Alghamdi, A.A., Asikin, M.N. "Progress on Modified Calcium Oxide Derived Waste-Shell Catalysts for Biodiesel Production", *Catalysts*, vol. 11, no. 194, 2021, pp. 1–26.
- [26] Marinkovic, M.M., Stojkovic, N.I., Vasic, M.B. Ljupkovic, R.B., Rancic, S.M., Spalovic, B.R. and Zarubica, A.R. "Synthesis of Biodiesel from Sunflower Oil Over Potassium Loaded Alumina as Heterogeneous Catalyst: The Effect of Process Parameters", *Hem. ind*, vol. 70, no. 6, 2016, pp. 639–648.
- [27] Ajala, E.O., Ajala, M.A., Ayinla, I.K., Sonusi, A.D. and Fanodun, S.E. "Nano-synthesis of Solid Acid Catalysts from Waste-iron-filling for Biodiesel Production using High Free Fatty Acid Waste Cooking Oil," *Sci. Rep.*, vol. 10, no. 13256, 2020c, pp. 1–21.
- [28] Xue, B., Luo, J., Zhang, F. and Fang, Z. "Biodiesel Production from Soybean and Jatropha Oils by Magnetic CaFe₂O₄–Ca₂Fe₂O₅-based Catalyst," *Energy*, vol. 68, 2014, pp. 584–591.
- [29] Okoye, C.C., Nwokedi, I.C. and Eije, O.C. "Biodiesel Synthesis from Waste Cooking Oil Using Periwinkle Shells as Catalyst," *J. Energy Res. Rev.*, vol. 4, no. 4, 2020, pp. 32–43.

- [30] Hsiao, M.C., Lin, C.C., Chang, Y.H. and Chen, L.C. "Ultrasonic Mixing and Closed Microwave Irradiation-assisted Transesterification of Soybean Oil", *Fuel*, vol. 89, no. 12, 2010, pp. 3618–3622.
- [31] Ang, G.T., Ooi, S.N., Tan, K.T., Lee, K. T. and Mohamed, A.R. "Optimisation and Kinetic Studies of Sea Mango (*Cerbera odollam*) Oil for Biodiesel Production via Supercritical Reaction", *Energy Convers. Manag.*, vol. 99, 2015, pp. 242–251.
- [32] Chowdhury, J., Cao, X., Al Basir, F. and Roy, P.K. "Effect of Mass transfer and Reaction Kinetics in Transesterification of Jatropha curcas oil", *Int. J. Math. Model. Methods Appl. Sci.*, vol. 11, 2017, pp. 130–138.
- [33] Hsiao, M., Hou, S., Kuo, J. and Hsieh, P. "Optimised Conversion of Waste Cooking Oil to Biodiesel using Calcium Methoxide as Catalyst under Homogenizer System Conditions," *Energies*, vol. 2622, 2018, pp. 1–12.
- [34] Kyari, M.Z., Danggoggo, S.M., Usman, B.B. and Muhammad, A.B. "Optimisation of Process Variables in the Biodiesel Production from *Lophira lanceolata* Seed Oil", *Niger. J. Basic Appl. Sci.*, vol. 25, no. 2, 2018, pp. 75-86.
- [35] Fayyazi, E., Ghobadian, B. van de Bovenkamp, H.H., Najafi, G., Hosseinzadehsamani, B., Heeres, H.J. and Yue, J. "Optimisation of Biodiesel Production over Chicken Eggshell-Derived CaO Catalyst in a Continuous Centrifugal Contactor Separator", *Ind. Eng. Chem. Res.*, vol. 57, 2018, pp. 12742–12755.
- [36] Gardy, J., Hassanpour, A., Lai, X., Ahmed, M.H. and Rehan, M. "Biodiesel Production from Used Cooking Oil using a Novel Surface Functionalised TiO₂ Nano-catalyst", *Appl. Catal. B Environ.*, vol. 207, 2017, pp. 297–310.
- [37] Ajala, E.O., Aberuagba, F., Olaniyan, A.M. and Onifade, K.R. "Comparative Study of Acid-base and Base Catalysed Process of Biodiesel Production," *J. Basic Appl. Res. Int.*, vol. 11, no. 2, 2015, pp. 87–96.
- [38] Obianke, M., Muhammad, A., Hassan, L., Aliero, A. and Liman, M. "Optimisation of

Reaction Variables In-situ Transesterification of *Jatropha curcas* Oilseed in Biodiesel," *Niger. J. Basic Appl. Sci.*, vol. 26, no. 2, 2018, pp. 102-114.